CrystEngComm

COMMUNICATION

View Article Online
View Journal | View Issue

Cite this: *CrystEngComm*, 2017, **19**, 5173

Received 20th June 2017,
Accepted 1st August 2017

DOI: 10.1039/c7ce01138e

rsc.li/crystengcomm

Supramolecular porphyrin-based metal–organic frameworks: Cu(II) naphthoate–Cu(II) tetrapyridyl porphine structures exhibiting selective CO_2/N_2 separation†

Tetsushi Ohmura, *[a] Norihiko Setoyama,[a] Yusuke Mukae,[a] Arimitsu Usuki,[a] Shunsuke Senda,[b] Tsuyoshi Matsumoto[c] and Kazuyuki Tatsumi[b]

1 and **2** were synthesized through the complexation of 5,10,15,20-tetra-4-pyridyl-21*H*,23*H*-porphine with copper(II) acetate and copper(II) 1-naphthoate and exhibited two-dimensional open and closed form structures, respectively. X-ray diffraction identified the supramolecular interactions leading to these packing motifs. N_2 and CO_2 sorption isotherms indicate that **2** allows the separation of these gases.

Introduction

Porphyrin-based metal–organic frameworks (P-MOFs) incorporating cavities have been widely studied in recent years. These compounds take advantage of the ability to accurately control the configuration of active sites, with anticipated applications in gas storage and catalysis, based on various combinations of transition metals and substituted organic ligands.[1] Further, advanced functional materials based on porphyrin assemblies have also been extensively studied.[2] One of the most versatile components for the construction of P-MOFs is 5,10,15,20-tetra-4-pyridyl-21*H*,23*H*-porphine (H_2TPyP). The tetragonal orientation of the peripheral pyridine ligands allows the formation of infinite parallel sheets with lattice structures in which four pyridyl groups are linked together by transition metal ions.[3]

Recently, we reported an example of a porous P-MOF comprised of H_2TPyP in a four-connected vertex with Cu paddlewheel clusters as linear linker motifs, forming regular 2 or 3-D coordination networks with an open format.[3d] As shown in Scheme 1, the H_2TPyP units are tetragonally connected *via* the Cu paddlewheel clusters in an infinite 2-D sheet structure with a 2.2 nm-wide square grid structure. Some P-MOFs exhibit very interesting properties that suggest potential applications, such as the selective sorption of gas molecules to modify CO_2 concentrations.[1d,4] We have therefore developed a strategy in which H_2TPyP and paddlewheel linkers are used to construct P-MOFs, increasing the potential for these materials to act as adsorbents exhibiting selectivity for CO_2/N_2. In this communication, we report the syntheses and characterizations of these P-MOFs.

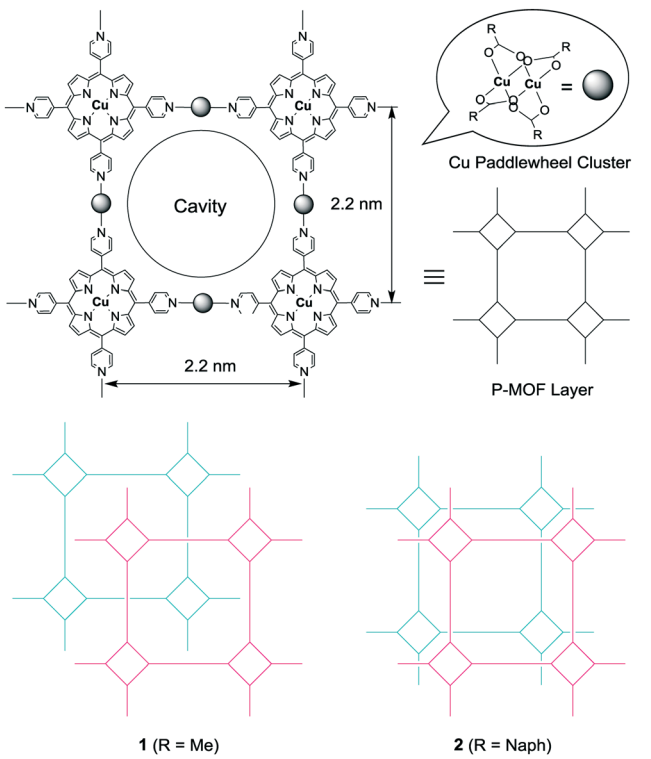

Scheme 1 Construction of P-MOFs incorporating cavities.

[a] *Toyota Central R&D Labs., Inc., 41-1, Yokomichi, Nagakute, Aichi 480-1192, Japan. E-mail: e1314@mosk.tytlabs.co.jp*
[b] *Research Center for Materials Science, Nagoya University, Furo-cho, Chikusa-ku, Nagoya, Aichi 464-8602, Japan*
[c] *Institute of Transformative Bio-Molecules (WPI-ITbM), Nagoya University, Furo-cho, Chikusa-ku, Nagoya, Aichi 464-8601, Japan*

† Electronic supplementary information (ESI) available: Single-crystal X-ray diffraction (XRD), thermal desorption mass spectrometry (TD-MS), and synchrotron powder XRD (PXRD) data. The CCDC numbers for the as-synthesized **1**, **2** and **CuNaph** are 1556754, 1556756 and 1556755. For ESI and crystallographic data in CIF or other electronic format see DOI: 10.1039/c7ce01138e

Experimental

Complexes **1** and **2** and **CuNaph** were synthesized and the products were confirmed by single-crystal X-ray diffraction (XRD). H_2TPyP was purchased from Aldrich, while copper(II) acetate ($Cu(OAc)_2$), 1-naphthoic acid (Naph), and the solvents (special grade) were purchased from Wako. The single crystal required for XRD analysis was prepared using a diffusion technique at room temperature. To synthesize **1**, a solution of $Cu(OAc)_2$ dissolved in methanol was carefully layered on top of a solution of H_2TPyP dissolved in chloroform. The resultant mixture was allowed to stand for 1–2 weeks, during which time reddish-brown crystals of the $Cu(OAc)_2$–CuTPyP (**1**) were formed. To obtain **2**, a solution of copper(II) 1-naphthoate (**CuNaph**) dissolved in ethanol was carefully layered onto a solution of H_2TPyP dissolved in chloroform. The resultant mixture was allowed to stand for 1–2 weeks, during which time dark-brown crystals of the CuNaph–CuTPyP (**2**) were formed. **CuNaph** was synthesized by layering a solution of $Cu(OAc)_2$ dissolved in methanol over top of a solution of Naph dissolved in ethyl acetate. The resultant mixture was allowed to stand for 1–2 weeks, during which time emerald green crystals of **CuNaph** were formed. Single-crystal XRD structural data were collected for **1**, **2**, and **CuNaph**. In preparation for these analyses, the crystals were first coated with a light hydrocarbon oil and then mounted on a loop in the nitrogen stream of the diffractometer. Diffraction data for the complexes were obtained under a cold N_2 stream using a Rigaku AFC8 equipped with a Saturn70 CCD detector for **1**, a Rigaku FR-E equipped with a Pilatus 200 K detector for **2**, and a Rigaku UltraX18 equipped with a Mercury CCD detector for **CuNaph**, employing graphite-monochromated Mo Kα radiation. The structure of **1** was solved by direct methods (SIR2014)[5] with the Crystal Structure crystallographic software package and refined by full-matrix least-squares procedures on F^2. The structure of **2** was solved by direct methods (SHELXL2013)[6] with the Crystal Structure crystallographic software package and refined by full-matrix least-squares procedures on F^2. The structure of **CuNaph** was solved by direct methods (SIR92)[7] with the Crystal Structure crystallographic software package and refined by full-matrix least-squares procedures on *F*. The SADI command was applied when modeling the disordered benzene rings of the 1-naphthoate moieties in **2**. The 1-naphthoate benzene rings in **2** were modelled as rigid groups using the EADP command. Non-hydrogen atoms were refined anisotropically, while hydrogen atoms were refined using the rigid model. In the case of **1** and **2**, the contribution of the solvent electron density was removed using the SQUEEZE routine in PLATON.[8] The final structures were validated using the PLATON cif check feature. The crystal data and structural refinement details are provided below and in the ESI.† Crystal data for **1**: tetragonal, $I4/mmm$ (#139), $a = b = 22.3460(7)$, $c = 14.2977(7)$ Å, $V = 7139.5(5)$ Å^3, $2\theta_{Max} = 55.1°$, $Z = 16$ and $R_1 = 0.0486$. Crystal data for **2**: monoclinic, $P2_1/c$ (#14), $a = 17.653(4)$, $b = 43.763(11)$, $c = 18.317(5)$ Å, $\beta = 102.967(3)°$, $V = 13\,790(6)$ Å^3, $2\theta_{Max} = 55.1°$, $Z = 4$ and $R_1 = 0.0987$. Crystal data for **CuNaph**: monoclinic, $P2_1/n$ (#14), $a = 13.918(5)$, $b = 8.908(3)$, $c = 17.689(7)$ Å, $\beta = 94.416(7)°$, $V = 2186.5(14)$ Å^3, $2\theta_{Max} = 54.9°$, $Z = 2$ and $R_1 = 0.0429$.

Results and discussion

The reaction of H_2TPyP and $Cu(OAc)_2$ produced reddish-brown crystals of **1** with a 2-D lattice structure (Fig. 1a). The 2-D sheets were interconnected through hydrogen bonds (2.693 Å) between H atoms on the methyl groups of one 2-D sheet and O atoms on the carboxylate moieties of an adjacent 2-D sheet (Fig. 1b). This value is shorter than the hydrogen bonds (2.828–2.954 Å) in $[MeC(O)N(H)PEt_3]_2[Cu_2(O_2C–Me)_4Cl_2]$.[9] Because the 2-D sheets in **1** do not interpenetrate, the channels that run through the structure can be used for gas absorption following evacuation of the P-MOF (Fig. 1c).[3d] In contrast, a combination of H_2TPyP and **CuNaph** generated brown crystals of **2**, also having a 2-D lattice structure (Fig. 2a). The **CuNaph** was synthesized from $Cu(OAc)_2$ and Naph, producing green crystals consisting of molecules having paddlewheel structures, using a procedure similar to that described in the literature.[10] Here, the 2-D sheets were interconnected through CH$\cdots\pi$ interactions (2.46–2.68 Å) between 1-naphthoate groups on the faces and edges of adjacent 2-D sheets (Fig. 2b). These value are shorter than the CH$\cdots\pi$ interactions (2.83–2.99 Å) in $[Cu_2(O_2CC_{14}H_9)_4(CH_3OH)_2]$.[10] Although the 2-D sheets in **2** do not interpenetrate, the channels in this material cannot be used for gas absorption because the pores are blocked by bulky 1-naphthoate ligands (Fig. 2c).

$CHCl_3$ solvent molecules initially filled the lattice cavities in **1**. The void fraction in the structure, estimated from the free volume to cell volume ratio after $CHCl_3$ was released from the open form structure using the van der Waals surface method,[11] was remarkably high at 0.67. This calculation assumes that the structure of the MOF skeleton did not change upon solvent removal due to the stabilizing effect of the hydrogen bonds between the 2-D sheets. The crystalline form of **2**, despite the closed form, was found to have a relatively small void fraction of 0.27.

The BET surface areas obtained for **1** and **2** from N_2 adsorption measurements at −196 °C were 812 and 1 m^2 g^{-1}, respectively, which correspond to essentially open and closed structural forms. However, **2** unexpectedly exhibited CO_2 adsorption at 0 °C. To examine selective CO_2 capture by **1** and **2**, CO_2 and N_2 sorption isotherms were acquired up to 100 kPa at 0 °C (Fig. 3). The isotherms for both at 0 °C demonstrate no uptake in the low concentration region but slowly increasing adsorption at higher concentrations. The materials were not saturated under these conditions, and the amount of CO_2 adsorbed by **2** was 0.349 mmol g^{-1} (15.3 mg g^{-1}), which was lower than the 1.49 mmol g^{-1} (65.5 mg g^{-1}) determined for **1**. However, the selectivity for CO_2/N_2 obtained from **2** was far superior to that of **1** (**2**: 49.6, **1**: 22.9). Here, the selectivity under adsorption conditions was calculated using the equation $\alpha_{12}{}^{ads} = (N_1{}^{ads}/N_2{}^{ads})(y_2/y_1)$

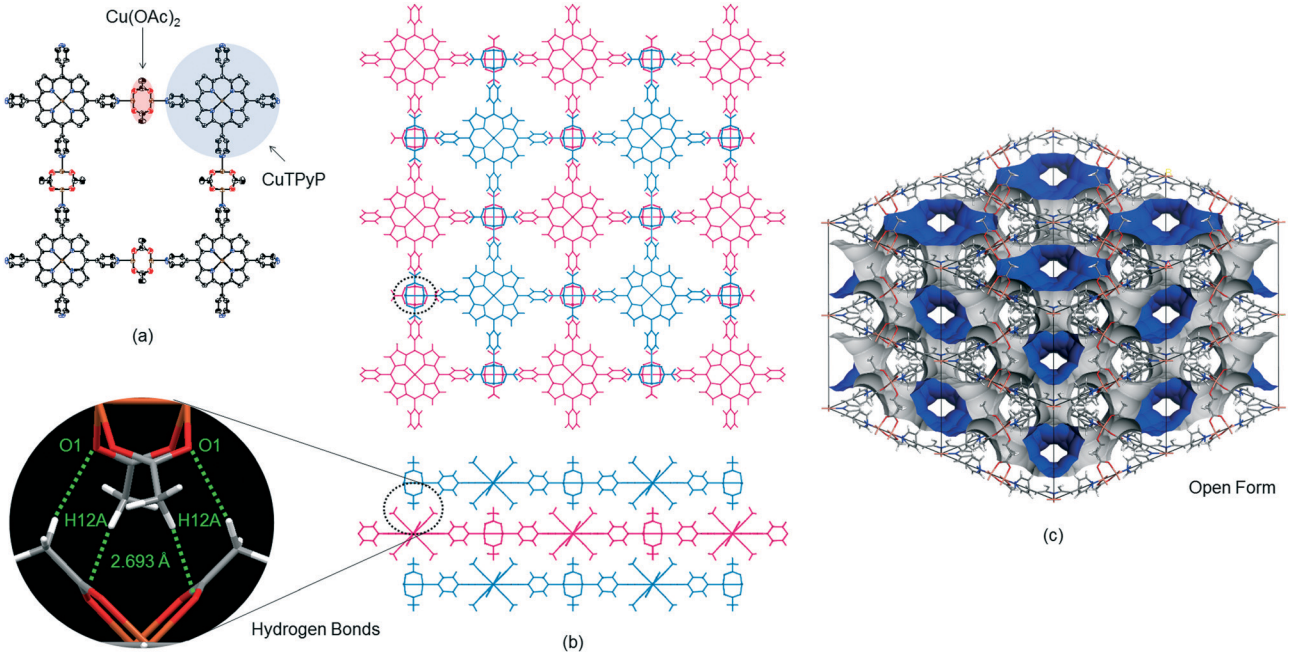

Fig. 1 (a) The 2.2 nm square grid of **1**. Color scheme: C = gray; N = blue; O = red; Cu = brown. For clarity, the solvent molecules are not shown. (b) The stacking of 2D sheets in **1**, with blue and red representing adjacent layers. (c) The crystal packing of **1** in the open form. For clarity, guest molecules and H atoms have been omitted.

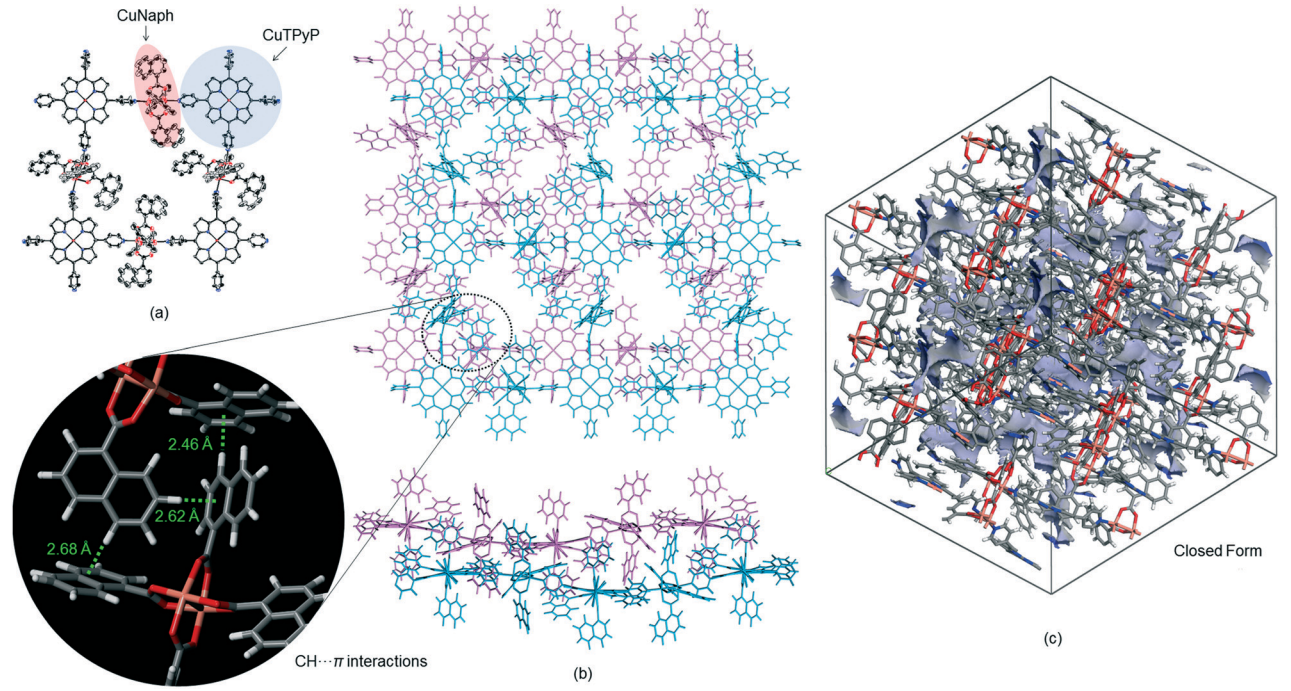

Fig. 2 (a) The 2.2 nm square grid of **2**. Color scheme: C = gray; N = blue; O = red; Cu = brown. For clarity, the solvent molecules are not shown. (b) The stacking of 2D sheets in **2**, with blue and red representing adjacent layers. (c) The crystal packing of **2** in the closed form. For clarity, guest molecules have been omitted.

described in the literature.[4e,12] The value obtained for 2 is comparable to those reported for various MOFs and zeolites.[4]

The closed-open transition is a vital aspect of the gas adsorption of these materials because the trigger for the transformation of the interaction between the host and guest determines the degree of selectivity. The observation that 2 adsorbs CO_2 but not N_2 shows that the selectivity results from the quadrupole moment or polarizability of the guest molecules, since both factors greatly affect the dispersion force of the guest.[13]

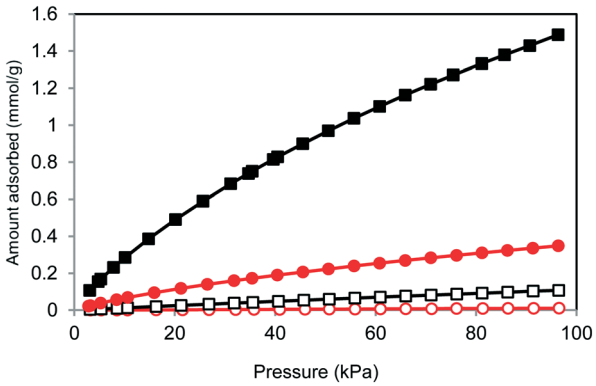

Fig. 3 CO_2 and N_2 adsorption isotherms for **1** and **2** at 0 °C (black squares, CO_2 for **1**; open squares, N_2 for **1**; red circles, CO_2 for **2**; open circles, N_2 for **2**).

Conclusions

We report 2-D P-MOFs constructed from Cu-based paddlewheel clusters and CuTPyP. Applications of these novel P-MOFs include the selective sorption of gas molecules. This study demonstrates that both P-MOFs and, in particular, compound **2** is a suitable candidate for selectivity for CO_2/N_2. We believe that this selective adsorption property can also be used for catalytic reaction. Furthermore, by using the limited reaction field of MOF, high selectivity can be expected. Further studies of catalytic activity for the conversion of CO_2 into useful chemicals are now in progress.

Acknowledgements

The synchrotron radiation experiments were performed on the BL22XU beamline at the SPring-8 facility with the approval of the Japan Synchrotron Radiation Research Institute (JASRI). The authors wish to thank Dr. Akihiko Machida for assistance with the experiments at Spring-8, Mr. Masami Yamamoto (Toyota Central R&D Laboratories, Inc.) for performing TD-MS analyses of **2**, and Mr. Yoshinori Idota (Toyota Central R&D Laboratories, Inc.) for performing the CO_2 adsorption measurements of **2**.

Notes and references

1 (*a*) S. Matsunaga, N. Endo and W. Mori, *Eur. J. Inorg. Chem.*, 2011, 4550; (*b*) T. R. Cook, Y.-R. Zheng and P. J. Stang, *Chem. Rev.*, 2013, **113**, 734, and references therein; (*c*) Q. Zha, C. Ding, X. Rui and Y. Xie, *Cryst. Growth Des.*, 2013, **13**, 4583; (*d*) W.-Y. Gao, M. Chrzanowski and S. Ma, *Chem. Soc. Rev.*, 2014, **43**, 5841, and references therein; (*e*) Q. Zha, X. Rui, T. Wei and Y. Xie, *CrystEngComm*, 2014, **16**, 7371, and references therein; (*f*) X. Rui, Q.-Z. Zha, T.-T. Wei and Y.-S. Xie, *Inorg. Chem. Commun.*, 2014, **48**, 111; (*g*) S. Matsunaga, N. Endo and W. Mori, *Chem. Lett.*, 2017, **46**, 937.

2 (*a*) P. Guo, P. Chen and M. Liu, *ACS Appl. Mater. Interfaces*, 2013, **5**, 5336; (*b*) P. Guo, G. Zhao, P. Chen, B. Lei, L. Jiang, H. Zhang, W. Hu and M. Liu, *ACS Nano*, 2014, **8**, 3402; (*c*) C. Zhang, P. Chen, H. Dong, Y. Zhen, M. Liu and W. Hu, *Adv. Mater.*, 2015, **27**, 5379; (*d*) G. Geng, P. Chen, B. Guan, L. Jiang, Z. Xu, D. Di, Z. Tu, W. Hao, Y. Yi, C. Chen, M. Liu and W. Hu, *ACS Nano*, 2017, **11**, 4866.

3 (*a*) C. V. K. Sharma, G. A. Broker, J. G. Huddleston, J. W. Baldwin, R. M. Metzger and R. D. Rogers, *J. Am. Chem. Soc.*, 1999, **121**, 1137; (*b*) L. Carlucci, G. Ciani, D. M. Proserpio and F. Porta, *Angew. Chem., Int. Ed.*, 2003, **42**, 317; (*c*) L. Carlucci, G. Ciani, D. M. Proserpio and F. Porta, *CrystEngComm*, 2005, **7**, 78; (*d*) T. Ohmura, A. Usuki, K. Fukumori, T. Ohta, M. Ito and K. Tatsumi, *Inorg. Chem.*, 2006, **45**, 7988; (*e*) L. D. DeVries and W. Choe, *J. Chem. Crystallogr.*, 2009, **39**, 229, and references therein; (*f*) R. W. Seidel and I. M. Oppel, *Struct. Chem.*, 2009, **20**, 121; (*g*) R. W. Seidel and I. M. Oppel, *CrystEngComm*, 2010, **12**, 1051; (*h*) R. W. Seidel and I. M. Oppel, *Z. Anorg. Allg. Chem.*, 2010, **636**, 446; (*i*) M.-H. Xie, X.-L. Yang, C. Zou and C.-D. Wu, *Inorg. Chem.*, 2011, **50**, 5318.

4 (*a*) R. V. Siriwardane, M.-S. Shen, E. P. Fisher and J. A. Poston, *Energy Fuels*, 2001, **15**, 279; (*b*) B. Wang, A. P. Côté, H. Furukawa, M. O'Keeffe and O. M. Yaghi, *Nature*, 2008, **453**, 207; (*c*) S. R. Miller, P. A. Wright, T. Devic, C. Serre, G. Férey, P. L. Llewellyn, R. Denoyel, L. Gaberova and Y. Filinchuk, *Langmuir*, 2009, **25**, 3618; (*d*) D. M. D'Alessandro, B. Smit and J. R. Long, *Angew. Chem., Int. Ed.*, 2010, **49**, 6058; (*e*) Y.-S. Bae and R. Q. Snurr, *Angew. Chem., Int. Ed.*, 2011, **50**, 11586; (*f*) S. Yang, X. Lin, W. Lewis, M. Suyetin, E. Bichoutskaia, J. E. Parker, C. C. Tang, D. R. Allan, P. J. Rizkallah, P. Hubberstey, N. R. Champness, K. M. Thomas, A. J. Blake and M. Schröder, *Nat. Mater.*, 2012, **11**, 710; (*g*) T. Bataille, S. Bracco, A. Comotti, F. Costantino, A. Guerri, A. Ienco and F. Marmottini, *CrystEngComm*, 2012, **14**, 7170; (*h*) G. E. Cmarik, M. Kim, S. M. Cohen and K. S. Walton, *Langmuir*, 2012, **28**, 15606; (*i*) T.-H. Bae, M. R. Hudson, J. A. Mason, W. L. Queen, J. J. Dutton, K. Sumida, K. J. Micklash, S. S. Kaye, C. M. Brown and J. R. Long, *Energy Environ. Sci.*, 2013, **6**, 128.

5 M. C. Burla, R. Caliandro, B. Carrozzini, G. L. Cascarano, C. Cuocci, C. Giacovazzo, M. Mallamo, A. Mazzone and G. Polidori, *J. Appl. Crystallogr.*, 2015, **48**, 306.

6 G. M. Sheldrick, *Acta Crystallogr., Sect. A: Found. Crystallogr.*, 2008, **64**, 112.

7 A. Altomare, G. Cascarano, C. Giacovazzo, A. Guagliardi, M. C. Burla, G. Polidori and M. Camalli, *J. Appl. Crystallogr.*, 1994, **27**, 435.

8 A. L. Spek, *J. Appl. Crystallogr.*, 2003, **36**, 7.

9 H. Ackermann, B. Neumüller and K. Dehnicke, *Z. Anorg. Allg. Chem.*, 2000, **626**, 1712.

10 M. Kyuzou, A. Maeda, M. Wada, S. Watanabe, T. Takei, T. Ohmura, Y. Kowaguchi, W. Mori and J. Tanaka, *Bull. Chem. Soc. Jpn.*, 2011, **84**, 491.

11 (*a*) D. Sun, F. S. Tham, C. A. Reed and P. D. W. Boyd, *Proc. Natl. Acad. Sci. U. S. A.*, 2002, **99**, 5088; (*b*) T. Ohmura, A. Usuki, Y. Mukae, H. Motegi, S. Kajiya, M. Yamamoto, S.

Senda, T. Matsumoto and K. Tatsumi, *Chem. – Asian J.*, 2016, **11**, 700.

12 N is the adsorbed amount and y is the molar fraction in the gas phase. Subscripts 1 and 2 indicate the strongly adsorbed component (CO_2) and the weakly adsorbed component (N_2), respectively. The ads superscripts mean adsorption conditions.

13 S. Shimomura, M. Higuchi, R. Matsuda, K. Yoneda, Y. Hijikata, Y. Kubota, Y. Mita, J. Kim, M. Takata and S. Kitagawa, *Nat. Chem.*, 2010, **2**, 633.